Available online at www.sciencedirect.com
ScienceDirect
Geochimica et Cosmochimica Acta 71 (2007) 3070–3081
Geochimica et Cosmochimica Acta
www.elsevier.com/locate/gca

The solubility of gold in hydrogen sulfide gas: An experimental study

Denis Yu. Zezin *, Artashes A. Migdisov, Anthony E. Williams-Jones

Department of Earth and Planetary Sciences, McGill University, 3450 University Street, Montreal, Que., Canada H3A 2A7

Received 20 December 2006; accepted in revised form 4 April 2007; available online 10 April 2007

Abstract

The solubility of gold in H_2S gas has been investigated at temperatures of 300, 350 and 400 °C and pressures up to 230 bars. Experimentally determined values of the solubility of Au are 0.4–1.4 ppb at 300 °C, 1–8 ppb at 350 °C and 8.6–95 ppb at 400 °C. Owing to a positive dependence of the logarithm of the fugacity of gold on the logarithm of the fugacity of H_2S, it is proposed that the solubility of Au can be attributed to formation of a solvated gaseous sulfide or bisulfide complex through reactions of the type:

$$\mathrm{Au(s)} + (n+1)\cdot \mathrm{H_2S(g)} = \mathrm{AuS}\cdot(\mathrm{H_2S})_n\mathrm{(g)} + \mathrm{H_2(g)} \tag{A}$$

or

$$\mathrm{Au(g)} + (n+1)\cdot \mathrm{H_2S(g)} = \mathrm{AuHS}\cdot(\mathrm{H_2S})_n\mathrm{(g)} + \tfrac{1}{2}\mathrm{H_2(g)} \tag{B}$$

which are f_{H_2}-dependent; n is a statistical solvation number. If the redox potential is buffered by S/H_2S (the case in our study), the corresponding reactions are:

$$\mathrm{Au(s)} + n\cdot \mathrm{H_2S(g)} + \mathrm{S(l)} = \mathrm{AuS}\cdot(\mathrm{H_2S})_n\mathrm{(g)} \tag{C}$$

or

$$\mathrm{Au(s)} + (n+\tfrac{1}{2})\cdot \mathrm{H_2S(g)} + \tfrac{1}{2}\mathrm{S(l)} = \mathrm{AuHS}\cdot(\mathrm{H_2S})_n\mathrm{(g)} \tag{D}$$

Values of n for these latter reactions were calculated to be 1.8 and 1.2 at 300 °C, 1.7 and 1.0 at 350 °C, 2.2 and 1.7 at 400 °C, respectively. The equilibrium constants for reactions C and D increase with temperature and have values of $\log K = -11.1 \pm 0.2$ at 300 °C (both reactions), -10.7 ± 0.3 and -10.5 ± 0.3 at 350 °C, and -10.6 ± 0.2 and -10.4 ± 0.2 at 400 °C, respectively. At the conditions of this study, the solubility of gold in H_2S gas is relatively high, and the results obtained provide strong evidence that H_2S can play an important role in the vapor transport of gold and the formation of hydrothermal gold deposits.

1. INTRODUCTION

Although there is now extensive evidence that the vapor phase in magmatic hydrothermal systems is capable of transporting high concentrations of some ore metals (see review in Williams-Jones and Heinrich, 2005), our understanding of how this transport occurs is still poor. The first experimental study to address this issue was that of Migdisov et al. (1999) who showed that at temperatures from 300 to 360 °C and pressures up to 180 bars the solubility of silver in H_2O–HCl vapors is orders of magnitude higher than predicted by simple volatility. They related this enhanced solubility to formation of the species $AgCl\cdot(H_2O)_n$. Archibald et al. (2001, 2002) reported even higher solubility of gold and copper in H_2O–HCl vapors at similar conditions and likewise interpreted their data as reflecting the

---

* Corresponding author. Fax: +1 514 398 4680.
E-mail address: zezin@eps.mcgill.ca (D.Yu. Zezin).

0016-7037/$ - see front matter © 2007 Elsevier Ltd. All rights reserved.
doi:10.1016/j.gca.2007.04.005

formation of hydrated chloride complexes ($AuCl \cdot (H_2O)_n$ and $Cu_xCl_x \cdot (H_2O)_n$). These latter studies measured concentrations of copper and gold in the vapor phase on the order of hundreds of ppm and tens of ppb, respectively, at a temperature of ~300 °C. By contrast, Heinrich et al. (1992, 1999) measured weight percent and ppm level concentrations of these metals, respectively, in higher temperature (>550 °C) vapor-rich fluid inclusions from magmatic ore deposits. Moreover, they showed that both metals partition preferentially into the vapor phase rather than into the coexisting brine. Based on this observation (i.e., that the concentrations of the metals do not correlate with chloride activity) and the fact that H_2S has a strong preference for the vapor phase, these authors proposed that the high concentrations of copper and gold in the vapor phase are due to their complexation with reduced sulfur.

The only experimental study to shed direct light on the ability of H_2S to complex with metals in the vapor phase is that of Zakaznova-Iakovleva et al. (2001), who showed that H_2S gas can dissolve significant concentrations of antimony as a result of the formation of the solvated species $Sb_2S_3 \cdot H_2S$. More recently, Pokrovski et al. (2006) have shown that the presence of sulfur may increase the partitioning of Au, Ag and Cu into the vapor phase at temperatures of up to 450 °C.

Inasmuch as complexes with HS^- and H_2S are the principal forms of dissolved gold in aqueous liquids (e.g., Hayashi and Ohmoto, 1991; Benning and Seward, 1996; Loucks and Mavrogenes, 1999; Stefansson and Seward, 2004; Tagirov et al., 2005) and H_2S partitions strongly into the vapor phase of hydrothermal systems, it is also likely that gaseous H_2S is an essential component in promoting the volatile transport of gold. In this paper, we report the results of an experimental study of the solubility of gold in hydrogen sulfide gas, and show that gold forms stable complexes with H_2S that serve to greatly increase its solubility over that predicted by the vapor pressure of metallic gold or even more volatile species like AuS. This study represents a first step towards understanding the behavior of gold in H_2S-bearing gases and is an essential step towards the quantitative modeling of gold transport and deposition in vapor-dominated hydrothermal systems.

2. METHOD

The method used in this study is identical to that described in previous experimental studies devoted to the transport of metals in the gas phase (e.g., Migdisov et al., 1999; Archibald et al., 2001, 2002; Zakaznova-Iakovleva et al., 2001; Migdisov and Williams-Jones, 2005; Rempel et al., 2006). The experiments were carried out in titanium-alloy autoclaves (Grade 2 and VT1-0) with volumes of ~40–50 cm^3. Autoclave volumes were determined by filling the autoclaves with 25 °C distilled water, and weighing them before and after filling. The weighing was performed to an accuracy of ±10 mg. After the autoclaves had been purged of atmospheric gases by passing nitrogen gas through them for about 30 min, they were cooled to a temperature of approximately −75 °C, and between 1 and 6 g of liquid H_2S was condensed in them from a stream of H_2S gas. The autoclaves were closed to the atmosphere during the introduction of the H_2S which was produced in a Kipp's type apparatus by the reaction

$$Na_2S + 2HCl = 2NaCl + H_2S$$

The H_2S gas was purified by passing it through two gas-washing bottles filled with nanopure water and then through a series of four cold traps (to remove condensable gases such as water vapor). As HCl has been shown to enhance the transport of gold in the gas phase (Archibald et al., 2001) and was one of the reagents used to produce H_2S, an aliquot of liquid from the second washing bottle was analyzed for its chloride content by HPLC (Activation Laboratories Ltd.). The concentration of this element was below the detection limit of the instrument (0.03 mg/L), and given that HCl partitions very strongly into the liquid phase, would have been even lower in the gas phase (NaCl was ignored as a possible contaminant because of its extremely low volatility). The cold traps cooled the H_2S to a temperature of −50 °C (using a mixture of dry CO_2 and methanol) and served to ensure removal of any H_2O introduced during washing (at this temperature the partial pressure of H_2O is ~10^{-5} bar) plus any condensable gases. Incondensable gases that might have remained after cleaning (e.g. HCl, which has a condensation temperature of −85 °C) would have been removed in the flow of gas exiting the autoclaves during the condensation of H_2S. The purity of H_2S produced and cleaned in the manner described above is considered to be ⩾99.8% by weight based on analyses reported in Migdisov et al. (1998).

A wire of native gold (Alfa Aesar, 99.95% purity) contained in a silica-glass holder was placed in each autoclave. In order to control the redox potential of the system, approximately 100 mg of powdered elemental sulfur (Alfa Aesar, 99.5% purity), which was sufficient to maintain equilibrium between H_2S gas and liquid sulfur at the conditions of the experiment according to reaction

$$H_2S(g) = S(l) + H_2(g)$$

was introduced into each autoclave in a separate open silica-glass holder. The holders were open at the top, and stood well above the liquid H_2S, thereby isolating the gold wire and native sulfur from the latter.

Experiments were performed at temperatures between 300 and 400 °C in an electric oven (Fisher Isotemp® models 818F and 550-126) equipped with an aluminum box (with a volume of about 0.05 m^3, the walls are about 1 cm thick), in which the autoclaves were placed, to reduce the temperature gradient. The choice of this range of temperatures was governed by the detection limit of the analytical method employed for gold analysis (at temperatures below 300 °C, the solubility of gold was expected to be too low to be measurable using instrumental neutron activation analysis, see below) and the critical temperature of sulfur (444.6 °C; Mills, 1974). The vertical temperature gradient, measured with two chromel–alumel thermocouples located at the top and bottom of the aluminum box, was generally less than 0.5 °C/m. A thermal regulator allowed the temperature to be controlled to an accuracy of ±1 °C. At the conditions of the experiments, the liquid H_2S was converted entirely to gas (the critical point of H_2S is at 100 °C and 89 bars), which filled the autoclaves and reacted with the solids in the silica-glass holders (Fig. 1). At the end of a set of experiments, the autoclaves were quenched to room temperature in a water bath and further cooled to a temperature of ~−75 °C in order to condense H_2S gas into liquid. The latter cooling ensured that, as was the case at the beginning of an experiment, gold wire and H_2S liquid were also spatially separated at the end of an experiment. The silica-glass holders containing sulfur and gold were then removed from the autoclaves and all the H_2S gas condensed into the liquid was released by slow boiling upon warming up the autoclave to room temperature. Sulfur-bearing holders were then weighed to determine the mass losses. Native sulfur and gold precipitated on the walls of the autoclaves during quenching were removed by washing with 1.5–3 mL of dilute (~10 wt%) nitric acid at a temperature of 200 °C and subsequently with 2–4 mL of aqua regia at room temperature (HNO_3 and HCl of Fisher Scientific Optima™ grade). The autoclaves were closed when heated in order to oxidize any native sulfur and other forms of reduced sulfur (e.g., polysulfanes, if present) that might have condensed on the walls and thereby ensure their complete dissolution in the washing solution (as sulfate). Washing of the walls of the autoclave was facilitated using a custom-designed rotating carousel that ensured semi-continuous contact of all the inner surfaces of the autoclave with the washing solution. The concentration of gold in the washing solutions, and hence dissolved in H_2S, was determined using instrumental neutron activation analysis (INAA) at Ecole Polytechnique (University of Montreal). The detection limit of the analytical technique was 0.1 ppb (1 ppb = 1 μg/L) and the precision was ±5% for samples with concentrations greater than 1 ppb and ±0.05 ppb for samples containing lower concentrations of Au. In order to ensure that no gold remained in the autoclaves after the first washing, the washing procedure was repeated and the resulting solutions also analyzed using INAA. The concentration of gold in these second-washing solutions was consistently below the detection limit, indicating that no gold was missed during the initial washing. The amount of sulfur transferred to the gas phase from the silica glass holder during an experiment was determined to an accuracy of ±0.1 mg by weighing the holders loaded with sulfur before and after each run.

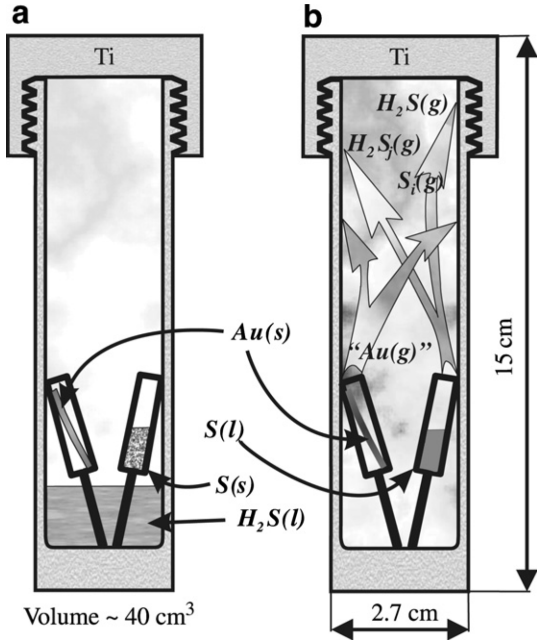

Fig. 1. Sketch of the experimental set-up. (a) Before an experiment, liquid H_2S gas is condensed in the autoclave at ~−75 °C and gold wire and sulfur powder are placed in silica-glass holders arranged in the autoclave so that the solids are not in contact with liquid H_2S. (b) As the autoclave is heated to the planned temperature of the experiment (300–400 °C), H_2S converts to gas, which reacts with the solids in the holders.

A series of blank experiments (three experiments at each temperature investigated) was conducted in an atmosphere free of hydrogen sulfide (i.e., nitrogen gas). The concentration of Au determined for these was below the detection limit of the analytical technique (0.1 ppb) indicating that there was no significant transport and precipitation of gold due simply to volatilization and condensation of the metallic gas.

The attainment of equilibrium was tested by means of a set of kinetic experiments of varying duration (from 1 to 22 days) at the lowest temperature investigated (300 °C). As the pressures in the autoclaves varied slightly (±10 bar) because of the difficulty in controlling the amount of H_2S condensed, it was, however, necessary to correct Au fugacities (their calculation is discussed below) to an arbitrarily chosen H_2S fugacity of 100 bars for purposes of comparison, (this was done using the dependencies of Au fugacity on the fugacity of H_2S gas determined from later experiments). The results of these kinetic runs are presented in Fig. 2 and show that reproducible (within 5%) Au fugacities were

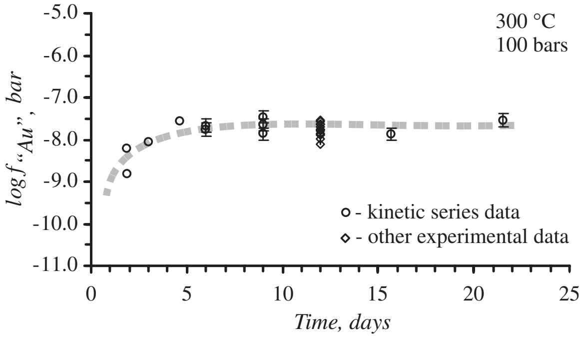

Fig. 2. Results of kinetic experiments at 300 °C and pressure normalized to 100 bars. Concentrations of the dissolved Au presented as $\log f_{\text{“Au(g)”}}$ were corrected to an arbitrarily chosen fugacity of H_2S of 100 bars because of the difficulty in maintaining the same pressure conditions for a full set of kinetic runs (the pressure in each autoclave was slightly different due to small differences in the amount of H_2S introduced into them). After 10 days, the system attained a plateau concentration interpreted to represent equilibrium. Comparison of the results of these and subsequent experiments suggests that the equilibrium concentration is reproducible to ±5% (see text for further explanation).

obtained in less than 10 days. Subsequent experiments were run for longer duration (>12 days), thereby ensuring that the measured metal concentrations closely approached the equilibrium concentrations.

3. RESULTS

The experiments were performed at temperatures of 300, 350 and 400 °C, and pressures varying from 25 to 230 bars. Owing to the very low vapor pressure of sulfur species in the experiment (typically less than 1 bar) and vanishingly small vapor pressure of gold ($<10^{-5}$ bar) compared to that of H_2S, the total pressure of the system was assumed to be equal to that of pure hydrogen sulfide. Pressure and fugacity coefficients were calculated using the accurately determined autoclave volume (minus the volume of the holders with gold wire and elemental sulfur), the mass of H_2S introduced and the equation of state for hydrogen sulfide gas (Rau and Mathia, 1982).

Assuming ideal behavior of volatile metal compounds, the fugacity of the gold-bearing compound was calculated using the ideal gas law, $f \cong P = nRT/V$, where P is the partial pressure of the gaseous Au complex, V is the volume of the autoclave, n the number of moles of Au dissolved in the gas phase (which was calculated from the concentration of Au measured in washing solutions and therefore represents the amount of Au transported from the gold wire to the gas phase), R the gas constant and T the temperature of the experiment. The results of the experiments are reported in Table 1 as logarithms of the fugacity of the gold-bearing gas species, $\log f_{\text{“Au(g)”}}$, and concentrations of gold dissolved in H_2S (ppb, i.e., μg per kg of H_2S). The solubility of Au in H_2S gas was found to range from 0.4 to 1.4 ppb at 300 °C, 1–8 ppb at 350 °C and 8.6–95 ppb at 400 °C

Table 1
The solubility of gold in H_2S gas

H_2S (mol)	Volume (cm^3)	P (bar)	ϕ	$\log f_{H_2S}$ bar	“Au(g)”[a] $\times 10^{11}$ mol	$\log f_{\text{“Au(g)”}}$[b] experimental	Au[c] (ppb)
300 °C							
0.041	37.75	49.0	0.95	1.67	0.36	−8.35	0.50
0.047	37.61	56.4	0.94	1.73	0.89	−7.95	1.1
0.048	37.56	57.7	0.94	1.74	0.71	−8.04	0.85
0.075	38.51	85.1	0.92	1.89	0.71	−8.06	0.55
0.073	36.88	86.3	0.92	1.90	0.71	−8.04	0.56
0.085	37.47	98.0	0.91	1.95	0.71	−8.04	0.48
0.088	37.55	101	0.90	1.96	0.53	−8.17	0.35
0.089	37.22	103	0.90	1.97	1.4	−7.74	0.92
0.109	38.26	120	0.89	2.03	2.1	−7.58	1.1
0.137	36.82	153	0.86	2.12	3.2	−7.38	1.3
0.159	37.73	171	0.85	2.16	2.3	−7.54	0.84
0.207	37.61	215	0.82	2.25	3.4	−7.37	0.94
350 °C							
0.020	37.10	26.9	0.98	1.42	0.36	−8.30	1.0
0.023	37.27	31.2	0.98	1.48	0.71	−8.01	1.8
0.043	37.06	57.3	0.96	1.74	0.71	−8.00	0.96
0.052	36.71	70.3	0.95	1.82	1.6	−7.65	1.8
0.066	36.77	87.4	0.94	1.91	1.6	−7.65	1.4
0.104	36.76	133	0.91	2.08	4.6	−7.19	2.6
0.140	36.94	174	0.88	2.19	4.3	−7.22	1.8
0.146	37.07	181	0.88	2.20	20	−6.55	8.0
0.188	37.21	228	0.86	2.29	5.3	−7.13	1.6
400 °C							
0.024	37.08	35.3	0.98	1.54	3.6	−7.27	8.6
0.024	36.94	35.4	0.98	1.54	5.0	−7.12	12
0.030	36.62	44.9	0.98	1.64	10	−6.80	20
0.045	37.28	65.1	0.96	1.80	45	−6.17	58
0.067	53.80	66.9	0.96	1.81	23	−6.62	20
0.063	38.56	87.9	0.95	1.92	104	−5.82	95
0.093	53.40	92.4	0.95	1.94	57	−6.22	36
0.128	54.30	126	0.94	2.07	82	−6.07	37
0.102	38.08	140	0.93	2.12	90	−5.88	51
0.152	53.40	148	0.93	2.14	83	−6.06	32
0.112	38.17	153	0.92	2.15	100	−5.84	51
0.118	38.33	159	0.92	2.17	122	−5.75	60
0.150	38.55	199	0.90	2.26	60	−6.06	23

[a] Amount of Au transported from the gold wire to the gas phase during the experiment.

[b] Calculated from the experimental data using ideal gas law (see text for explanation).

[c] The solubility of Au in H_2S gas in the experiments presented as ppb = μg/kg.

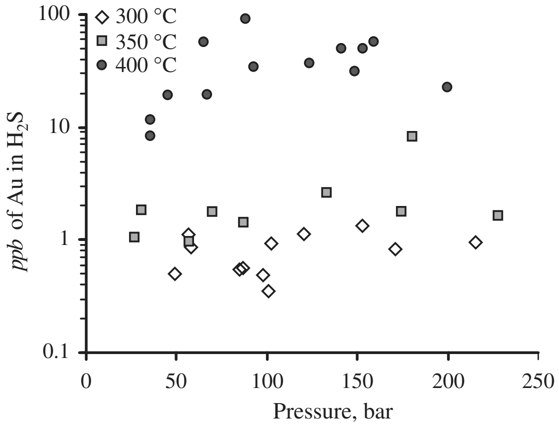

Fig. 3. A plot of the concentration of Au (in ppb or μg/kg) dissolved in H_2S gas versus pressure at the conditions of the solubility experiments (temperatures of 300, 350 and 400 °C and pressures of 25–230 bars).

(Fig. 3) and a positive correlation of $\log f_{\text{“}Au(g)\text{”}}$ with $\log f_{H_2S(g)}$ was observed at all temperatures investigated (see Fig. 7 and discussion below).

4. DISCUSSION

4.1. The solubility of Au in H_2S gas

Thermochemical properties of the following gaseous species of gold, Au, AuH and AuS, are reported in Mills (1974) and Binnewies and Milke (1999). Evidence for the existence of the molecule Au_2S(g) was reported by Smoes and Drowart (1968), however no information was provided on its stability, and it is not considered in our calculations. Calculations based on the available thermodynamic data show that, among these species, only AuS(g) is likely to play a significant role in the vapor transport of gold (Symonds and Reed, 1993; Taran et al., 2000). We therefore initially attempted to describe the solubility of gold in H_2S gas solely in terms of this species and an assumption that there are no interactions between the solvent (H_2S gas) and AuS(g), i.e., that the behavior of the latter is ideal. The experimental system was assumed to contain the following compounds: native gold, Au(g), AuS(g), S(l), S_i(g), H_2S(g), H_2S(l), H_2S_j(g), and H_2S_k(l), where *i* (representing gaseous sulfur polymers) varies from 1 to 8 (Rau et al., 1973), *j* (representing gaseous hydrogen polysulfanes) varies from 2 to 6 (Féher and Winkhaus, 1957; Migdisov et al., 1998), and *k* (representing liquid polysulfanes) is greater than 1 (Steudel, 2003). A variety of gaseous and liquid hydrogen polysulfanes are likely to have formed as a result of the interaction of sulfur with H_2S and, as will be shown below, influence the mass balance of sulfur in the system (Migdisov et al., 1998; Steudel, 2003) as well as complicate the final gold fugacity calculations.

The solubility of gold in the vapor phase was described initially by the following reaction:

$$\mathrm{Au(s) + H_2S(g) = AuS(g) + H_2(g)} \qquad (1)$$

This reaction is dependent on $f_{H_2(g)}$. However, when combined with the reaction

$$\mathrm{H_2(g) + S(l) = H_2S(g)} \qquad (2)$$

it yields the reaction

$$\mathrm{Au(s) + S(l) = AuS(g)} \qquad (3)$$

which depends instead on the activity of liquid sulfur. In order to quantitatively estimate the equilibrium constant for reaction (1) or (3), and hence, to obtain values of the solubility of Au in H_2S gas, it is essential to know either the fugacity of hydrogen gas or the activity of liquid sulfur at equilibrium (both effectively represent the same redox equilibria). Owing to the difficulty in determining $f_{H_2(g)}$ at the experimental conditions, it was necessary to evaluate the solubility of Au in H_2S gas using the activity of liquid sulfur and reaction (3).

4.2. Activity of liquid sulfur in the system S–H_2S

Owing to the appreciable consumption of H_2S gas that occurs during its interaction with molten sulfur (Fanelli, 1949), the activity of liquid sulfur cannot be assumed to be equal to unity. Moreover, evaluation of this activity is complicated by the fact that the consumption of H_2S, as first suggested by Fanelli (1949) and subsequently demonstrated by Wiewiorowski and Touro (1966), is due not only to simple dissolution of H_2S but also to the formation of liquid polysulfanes (H_2S_k), via the reaction

$$\mathrm{H_2S(g)} + (k-1)\cdot \mathrm{S(l)} = \mathrm{H_2S}_k(l) \qquad (4)$$

Wiewiorowski and Touro (1966) showed, furthermore, that the solubility of H_2S gas in molten sulfur actually decreases with increasing temperature and that at temperatures above about 150 °C, formation of polysulfanes predominates over simple dissolution of H_2S (Fig. 4). The dissolution of H_2S

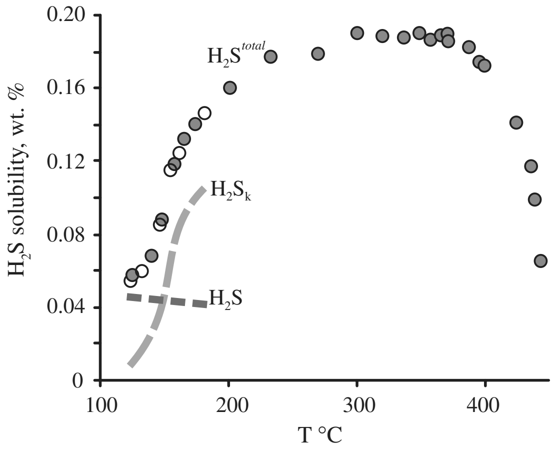

Fig. 4. The solubility of hydrogen sulfide gas in liquid sulfur. The data are from the solubility experiments of Fanelli (1949; closed circles) and Wiewiorowski and Touro (1966; open circles). The net contributions of the species H_2S and H_2S_k to the total solubility of hydrogen sulfide (H_2S^{total}) in sulfur melt were measured using direct infrared spectroscopy by Wiewiorowski and Touro (1966) and are shown by the black and grey dashed lines, respectively.

gas into the sulfur melt and the formation of polysulfane species result in a decrease in the mole fraction, and hence activity, of liquid sulfur.

Inasmuch as the only experimental data available on the stability of liquid polysulfanes in the melt are for temperatures below 180 °C (Wiewiorowski and Touro, 1966), neither the values for the mole fraction of liquid sulfur in the melt nor the corresponding activity coefficients are known at the temperatures considered in our experiments (300–400 °C). On the other hand, the volatility of sulfur species and thus the amount of sulfur that can be transported in the gas phase are related to the activity of liquid sulfur through the following reactions:

$$iS(l) = S_i(g), \quad K_{(5)} = \frac{f_{S_i(g)}}{a^i_{S(l)}} \tag{5}$$

and

$$H_2S(g) + (j-1)\cdot S(l) = H_2S_j(g), \quad K_{(6)} = \frac{f_{H_2S_j(g)}}{f_{H_2S(g)}\cdot a^{j-1}_{S(l)}} \tag{6}$$

As the equilibrium constants for these reactions can be calculated from thermodynamic data (Mills, 1974; Suleimenov and Ha, 1998), it is thus possible to use them to extract values of the activity of S(l) in the melt by determining the amount of sulfur transported into the gas phase coexisting with the melt. However, given that there are no data on the fugacity coefficients of the different sulfur species in the gas phase, it is necessary to assume that they are equal to their corresponding partial pressures and thus that

$$P_{S_i(g)} \cong f_{S_i(g)} = K_{(5)}\cdot a^i_{S(l)} \tag{7}$$

and

$$P_{H_2S_j(g)} \cong f_{H_2S_j(g)} = K_{(6)}\cdot f_{H_2S(g)}\cdot a^{j-1}_{S(l)} \tag{8}$$

The mass of sulfur transported into the gas phase was therefore calculated from the ideal gas law

$$n = \frac{P^{\text{total}}_{S(g)}V}{RT}$$

where n is the number of moles of sulfur lost from the holder during the experiment, V is the effective volume of the autoclave, R the gas constant and T the temperature of the experiment. The activity of liquid sulfur was in turn determined using the relationship

$$\text{mol}^{\text{total}}_{S(g)} = \left(\sum_{i=1}^{8} i\cdot K_{S_i}\cdot a^i_{S(l)} + \sum_{j=2}^{6} K_{H_2S_j}\cdot f_{H_2S(g)}\cdot a^{j-1}_{S(l)}\right)\cdot\frac{V}{RT} \tag{9}$$

The values of K_{S_i} and $K_{H_2S_j}$ were calculated from Mills (1974) and Suleimenov and Ha (1998), respectively, the value for $f_{H_2S(g)}$ was evaluated from the equation of state for H_2S (Rau and Mathia, 1982), V is the known volume of the autoclave, T is the temperature of the experiment and $\text{mol}^{\text{total}}_{S(g)}$ is the mass loss of sulfur determined experimentally. Eq. (9) thus has only one unknown, namely the activity of liquid sulfur, $a_{S(l)}$, and could therefore be solved for this parameter. It should be noted, however, that as the activity coefficient of liquid sulfur in the melt is unknown, this solution did not provide any information on the mole fraction of sulfur in the melt or further constrain the composition of the latter.

From Fig. 5 it is evident that the activity of liquid sulfur in the melt decreases with increasing $f_{H_2S(g)}$ due to the dissolution of H_2S gas and the resultant formation of liquid polysulfanes. However, the extent to which $a_{S(l)}$ decreases depends on temperature. For example, between 300 and 350 °C, $a_{S(l)}$ decreases to 0.47, whereas at 400 °C it only decreases to 0.7 (Fig. 5), which is consistent with the observation of Fanelli (1949) that the total solubility of H_2S in molten sulfur reaches a broad maximum (plateau value) between 300 and 370 °C (Fig. 4). Another pertinent observation is that the cumulative partial pressure of gaseous hydrogen polysulfanes exceeds that of gaseous elemental sulfur species at fugacities of H_2S gas above about 20 bars (Fig. 6), which agrees well with the findings of Migdisov et al. (1998), who showed that the solubility of sulfur in H_2S gas at temperatures above 200 °C can be attributed entirely to the formation of gaseous hydrogen polysulfanes.

4.3. The solubility of Au as AuS(g)

Having determined the activity of liquid sulfur, the fugacity of AuS(g) was calculated from the expression for reaction (3), the equilibrium constant of which is given by

$$\log K_{(3)} = \log f_{AuS(g)} - \log a_{S(l)} - \int_{P_1}^{P_2}\frac{V^\circ}{RT}\,dp \tag{10}$$

The equilibrium constant, $K_{(3)}$, was calculated from standard thermodynamic data (Mills, 1974), the activity of liquid sulfur $a_{S(l)}$ was obtained from Table 2, V° is the sum of the molar volumes of native gold and sulfur, and R is the gas constant. The last term of the equation is the Poynting pressure correction (Sandler, 1989). However, over the range of conditions at which the experiments were

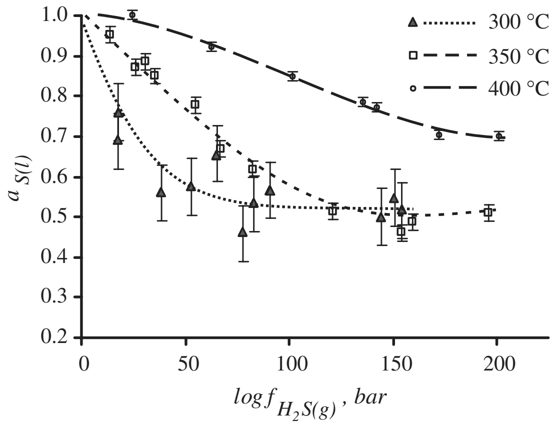

Fig. 5. The activity of S in molten sulfur as a function of the fugacity of H_2S in the system. A polynomial equation (Table 3) fitted to the experimental data at 300, 350 and 400 °C (with 1σ standard deviations of ±0.07, ±0.02 and ±0.01, respectively) was used to calculate the activity of molten sulfur at the conditions of interest (see text for further explanation).

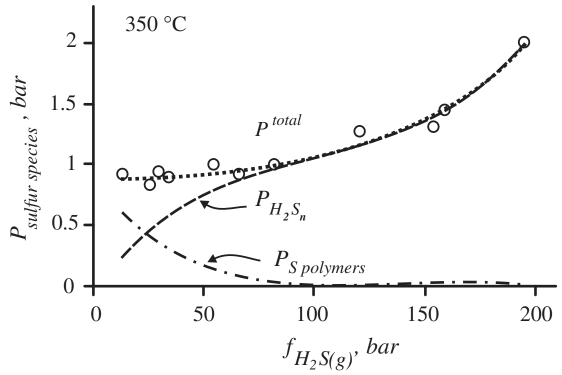

Fig. 6. The sum of the partial pressures of gaseous sulfur species (S_i and H_2S_j) as a function of the fugacity of H_2S gas. Circles represent the cumulative partial pressure of sulfur species determined in the experiments. The partial pressures of gaseous polysulfanes (dashed line) and sulfur polymers (dashed–dotted line) were calculated from the thermodynamic data taking into account the variable activity of sulfur with respect to the fugacity of H_2S gas (see text for details). At a pressure above about 20 bars, hydrogen polysulfanes replace sulfur polymers as the dominant form of sulfur in H_2S gas and at pressures above 70 bars are the principal form of dissolved sulfur in the gas phase.

conducted, corrections provided by this term do not exceed 0.05, which is much lower than the experimental error, and therefore can be ignored. The values of gold solubility in H_2S gas calculated using Eq. (10) are presented in Table 3 (as $\log f_{\text{“}Au(g)\text{”}}$) and illustrated in Fig. 7.

As is evident from Fig. 7, there are significant discrepancies between the calculated values of $\log f_{\text{“}Au(g)\text{”}}$ and those determined experimentally. The calculated values are 10^3–10^4 lower at 300 °C, $10^{1.5}$–10^3 lower at 350 °C and 10–10^3 lower at 400 °C. Furthermore, unlike the experimental data, the calculated fugacity of gaseous gold species does not correlate positively with the fugacity of H_2S gas. These observations indicate clearly that the formation of gaseous AuS cannot alone be responsible for the solubility of gold in H_2S gas.

4.4. Au dissolution as a solvated species

The positive dependence of the dissolved gold concentration on the fugacity of H_2S gas suggests that gold solubility may be controlled in part by a solvated species resulting from solute–solvent interaction. By analogy with models developed for solid–H_2O (vapor) systems (Migdisov et al., 1999; Archibald et al., 2001, 2002; Migdisov and Williams-Jones, 2005; Rempel et al., 2006), we propose that this species has the form of an uncharged solvated gaseous complex with reduced sulfur, e.g., $AuS \cdot (H_2S)_n$ or $AuHS \cdot (H_2S)_n$, resulting from reactions of the type

$$Au(s) + (n+1) \cdot H_2S(g) = AuS \cdot (H_2S)_n(g) + H_2(g) \quad (11)$$

$$Au(s) + (n+1) \cdot H_2S(g) = AuHS \cdot (H_2S)_n(g) + \tfrac{1}{2}H_2(g) \quad (12)$$

where n is the solvation number of the gold species or the number of H_2S molecules in a shell immediately adjacent to a gold-bearing species held there by van der Waals bonding (akin to a hydration shell). Even though this number represents a statistical approximation and is dependent on both temperature and pressure, we still can consider reactions Eqs. (11) and (12) as being stoichiometric based on the fairly good assumption that within the experimental range of pressures the solvation number is pressure-independent. This allows us to calculate the solvation number and the equilibrium constant for the solubility reaction in the manner described by Migdisov et al. (1999).

Unfortunately, we cannot distinguish between the above species based on the experimental data reported earlier. However, as AuS(g) is the most stable known gold species in the Au–H–S gas system, it is reasonable to propose that the gaseous volatile complex responsible for the high solubility of gold in H_2S gas has the form $AuS \cdot (H_2S)_n$. It is equally possible, given the importance of AuHS° species in aqueous liquids (e.g., Stefansson and Seward, 2004), that the species controlling gold solubility in H_2S gas has the form $AuHS \cdot (H_2S)_n$. In the following paragraphs we evaluate formation constants for these two species.

As discussed above, hydrogen fugacity is related to the activity of liquid sulfur and fugacity of H_2S gas in the system through reaction (2). Therefore, by combining reactions (2) and (11) and reactions (2) and (12) we obtain the following reactions describing equilibrium in the system

$$Au(s) + n \cdot H_2S(g) + S(l) = AuS \cdot (H_2S)_n(g) \quad (13)$$

$$Au(s) + \left(n+\tfrac{1}{2}\right) \cdot H_2S(g) + \tfrac{1}{2}S(l) = AuHS \cdot (H_2S)_n(g) \quad (14)$$

The equations for the equilibrium constants of these reactions are

$$\log K_{(13)} = \log f_{AuS\cdot(H_2S)_n(g)} - \log a_{S(l)} - n \cdot \log f_{H_2S(g)} \quad (15)$$

$$\log K_{(14)} = \log f_{AuHS\cdot(H_2S)_n(g)} - \tfrac{1}{2} \cdot \log a_{S(l)} - \left(n+\tfrac{1}{2}\right) \cdot \log f_{H_2S(g)}, \text{ respectively} \quad (16)$$

The procedure used to determine the solvation number of the gaseous complex was similar to that employed in previous investigations of metal transport by vapor (Migdisov et al., 1999; Archibald et al., 2001, 2002; Zakaznova-Iakovleva et al., 2001; Migdisov and Williams-Jones, 2005; Rempel et al., 2006). However, unlike the dependencies of

Table 2
Coefficients for the polynomial equation employed to estimate the activity of liquid sulfur ($a_{S(l)}$)

T (°C)	$a_{S(l)} = a + b \cdot f_{H_2S(g)} + c \cdot f^2_{H_2S(g)} + d \cdot f^3_{H_2S(g)}$				
	a	b	c	d	±1σ
300	0.8980	$-7.49 \cdot 10^{-3}$	$3.37 \cdot 10^{-5}$		±0.07
350	1.0108	$-4.67 \cdot 10^{-3}$	$-6.47 \cdot 10^{-6}$	$9.15 \cdot 10^{-8}$	±0.02
400	1.0041	$-1.16 \cdot 10^{-4}$	$-2.07 \cdot 10^{-5}$	$6.82 \cdot 10^{-8}$	±0.01

Table 3
Calculated fugacities of gaseous gold species based on experimental data reported in this study compared with values calculated from published thermodynamic data (The activity of sulfur was calculated from the polynomial equations given in Table 2)

P (bar)	$\log f_{H_2S(g)}$ (bar)	$a_{S(l)}$	$\log f_{\text{“Au(g)”}}$[a] calculated as AuS(g)	$\log f_{\text{“Au(g)”}}$[b] experimental	$\log f_{\text{“Au(g)”}}$[c] modeled as $AuS \cdot (H_2S)_n$
300 °C					
49.0	1.67	0.63	−11.62	−8.35	−8.35
56.4	1.73	0.60	−11.65	−7.95	−8.26
57.7	1.74	0.60	−11.65	−8.04	−8.25
85.1	1.89	0.52	−11.71	−8.06	−8.00
86.3	1.90	0.52	−11.72	−8.04	−8.00
98.0	1.95	0.50	−11.73	−8.04	−7.92
101	1.96	0.49	−11.74	−8.17	−7.90
103	1.97	0.49	−11.74	−7.74	−7.89
120	2.03	0.47	−11.76	−7.58	−7.78
153	2.12	0.49	−11.75	−7.38	−7.62
171	2.16	0.52	−11.74	−7.54	−7.54
215	2.25	0.66	−11.67	−7.37	−7.34
350 °C					
26.9	1.42	0.88	−9.83	−8.30	−8.30
31.2	1.48	0.86	−9.84	−8.01	−8.21
57.3	1.74	0.75	−9.89	−8.00	−7.84
70.3	1.82	0.70	−9.92	−7.65	−7.72
87.4	1.91	0.64	−9.96	−7.65	−7.60
133	2.08	0.51	−10.04	−7.19	−7.38
174	2.19	0.47	−10.07	−7.22	−7.22
181	2.20	0.47	−10.07	−6.55	−7.20
228	2.29	0.53	−10.01	−7.13	−7.03
400 °C					
35.3	1.54	0.98	−8.42	−7.27	−7.13
35.4	1.54	0.98	−8.42	−7.12	−7.12
44.9	1.64	0.96	−8.43	−6.80	−6.91
65.1	1.80	0.93	−8.44	−6.17	−6.57
66.9	1.81	0.93	−8.44	−6.62	−6.55
87.9	1.92	0.89	−8.45	−5.82	−6.31
92.4	1.94	0.88	−8.46	−6.22	−6.26
126	2.06	0.82	−8.48	−6.07	−6.01
140	2.12	0.79	−8.50	−5.88	−5.91
148	2.14	0.77	−8.50	−6.06	−5.86
153	2.15	0.77	−8.51	−5.84	−5.84
159	2.17	0.76	−8.51	−5.75	−5.80
199	2.26	0.71	−8.53	−6.06	−5.62

[a] Calculated from thermodynamic data using reaction (C): $Au(s) + S(l) = AuS(g)$.
[b] Calculated from experimental data.
[c] Modeled from experimental data for reaction (13): $Au(s) + n \cdot H_2S(g) + S(l) = AuS \cdot (H_2S)_n(g)$.

$\log f_{\text{“Me(g)”}}$ on $\log f_{\text{gas–solvent}}$, which were linear in these studies, the dependency in the present case is nonlinear due to the variable activity of liquid sulfur. The solvation number n and equilibrium constant for reactions Eqs. (13) and (14) were calculated iteratively using MATLAB® software from initial guesses and progressive minimization of the function U

$$U = \sqrt{\sum \left(\frac{f^{\text{exp}} - f^{\text{model}}}{f^{\text{model}}} \right)^2}, \tag{17}$$

where f^{exp} is the fugacity of the gold-bearing gaseous complex calculated from experimental data using assumptions discussed above, f^{model} is the modeled fugacity of the corresponding gaseous complex ($AuS \cdot (H_2S)_n$ or $AuHS \cdot (H_2S)_n$) at each fugacity of H_2S investigated. The term f^{model} was evaluated using the solvation number and the equilibrium constant for the corresponding complexation reaction (i.e., for the formation of $AuS \cdot (H_2S)_n$ or $AuHS \cdot (H_2S)_n$), which were used as adjustable parameters in the iteration procedure. The algorithm employed in the minimization was the Nelder–Mead simplex search described by Nelder and Mead (1965) and Dennis and Woods (1987).

The equilibrium constant for the reaction describing the formation of the gaseous gold-bearing complex increases with increasing temperature from 300 to 400 °C (Table 4). The solvation number (referred to below as $n_{(13)}$ and $n_{(14)}$ in reactions (13) and (14), respectively), however, is higher at 400 °C ($n_{(13)} = 2.2$, $n_{(14)} = 1.7$), than at 300 and 350 °C ($n_{(13)} = 1.8$ and 1.7 and $n_{(14)} = 1.2$ and 1,

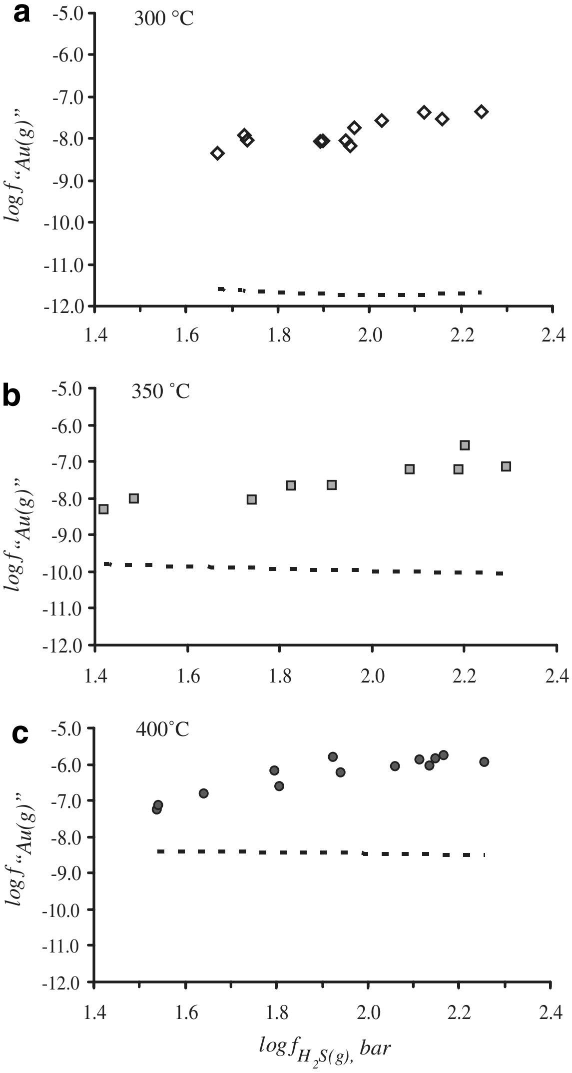

Fig. 7. A plot of log$f_{\text{“Au(g)”}}$ versus log $f_{H_2S(g)}$ comparing the experimentally determined fugacity of dissolved gold to that predicted assuming that this fugacity is dependent entirely on the formation of gaseous gold sulfide AuS(g) (dashed line). The calculated values are 10^3–10^4 lower at 300 °C (a), $10^{1.5}$–10^3 lower at 350 °C (b) and 10–10^3 lower at 400 °C (c). Unlike the experimental data, the calculated fugacity of gaseous gold species does not correlate positively with the fugacity of H_2S gas (solid lines reflect the positive trend of the dependence of log$f_{\text{“Au(g)”}}$ on log $f_{H_2S(g)}$; see text for further explanation).

respectively), which is unusual for gaseous metallic species. In contrast to metallic species in H_2O and H_2O–HCl gases (Williams-Jones et al., 2002 and references therein; Migdisov and Williams-Jones, 2005; Rempel et al., 2006), the dependence of the fugacity of the gaseous gold complex on the total fugacity of H_2S gas (Table 3) is slightly nonlinear due to the effect of the change in the activity of liquid sulfur with $f_{H_2S(g)}$ (Fig. 8). This deviation from nonlinearity is more pronounced at temperatures of 300 and 350 °C than at 400 °C due to the much lower plateau values of $a_{S(l)}$ with increasing $f_{H_2S(g)}$.

Table 4
Values of the solvation number, n, $\log K_{(13)}$ and $\log K_{(14)}$ for the reactions $Au(s) + n \cdot H_2S(g) + S(l) = AuS \cdot (H_2S)_n(g)$ and $Au(s) + (n + \frac{1}{2}) \cdot H_2S(g) + \frac{1}{2}S(l) = AuHS \cdot (H_2S)_n(g)$ calculated using the minimization function given by Eq. (17)

T (°C)	$AuS \cdot (H_2S)_n(g)$		$AuHS \cdot (H_2S)_n(g)$	
	$n_{(13)}$	$\log K_{(13)}$	$n_{(14)}$	$\log K_{(14)}$
300	1.8	-11.1 ± 0.2[a]	1.2	-11.1 ± 0.2
350	1.7	-10.7 ± 0.3	1.0	-10.5 ± 0.3
400	2.2	-10.6 ± 0.2	1.7	-10.4 ± 0.2

[a] The uncertainty represents the standard deviation for the experimental data ($\pm 1\sigma$).

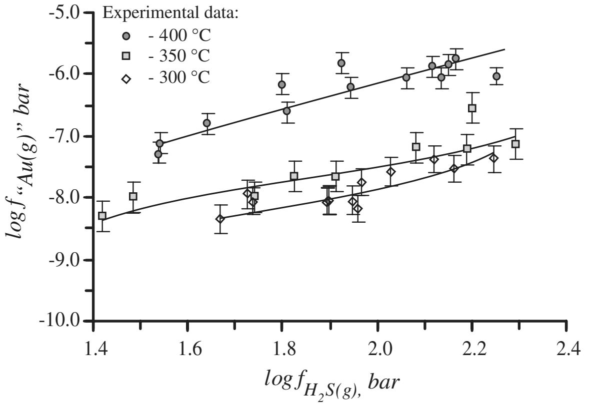

Fig. 8. A plot of the experimentally determined solubility of Au in H_2S gas at temperatures of 300 °C (a), 350 °C (b) and 400 °C (c). The solid lines represent the values calculated in this study for the solubility of the gaseous species, $AuS \cdot (H_2S)_n$ or $AuHS \cdot (H_2S)_n$ (n varying from 1 to 2.2 at temperatures between 300 and 400 °C, see text for details). The nonlinear dependence of the calculated solubility of Au in H_2S gas is due to the deviation of $a_{S(l)}$ from unity.

4.5. Comparison to previous studies

The only previous study to investigate the solubility of metals in H_2S gas is that of Zakaznova-Iakovleva et al. (2001). Using an approach similar to that described in our study, the authors concluded that the solubility of stibnite (Sb_2S_3) in H_2S gas is due to the formation of the solvated gaseous complex $Sb_2S_3 \cdot (H_2S)$. Comparing the solubility isotherms presented in that study with those obtained in our study, it is clear that, despite the substantially greater solubility of stibnite, their form is essentially the same, reflecting a very similar process of solvation of metal-bearing species by H_2S gas molecules (Fig. 9).

Although direct comparison of the results of this study to those obtained previously for H_2O–HCl mixtures (Archibald et al., 2001) is difficult, it is worth noting that the solubility of Au in H_2S gas is about one to two orders of magnitude greater than that obtained for Au in the system H_2O–HCl at similar conditions (Fig. 10). It is also worth noting that gold solubility in the H_2O–HCl system is retrograde at temperatures above 300 °C, whereas the stability of gold species in H_2S increases appreciably with

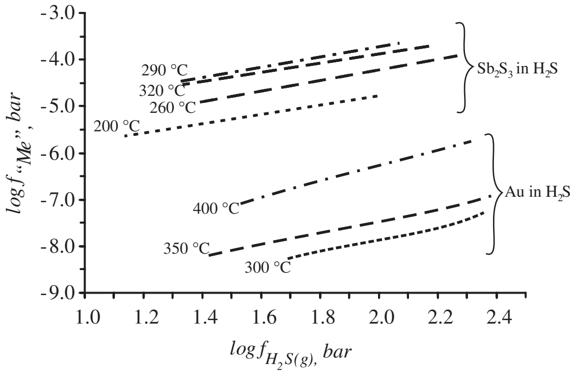

Fig. 9. A comparison of the solubility of gold in H_2S gas determined in this study (as $AuS \cdot (H_2S)_n$ or $AuHS \cdot (H_2S)_n$ with $n = 1$–2.2 at $T = 300$–400 °C) with the solubility of stibnite (Sb_2S_3) in H_2S (as $Sb_2S_3 \cdot (H_2S)$at $T = 300$–360 °C) measured by Zakaznova-Iakovleva et al., 2001.

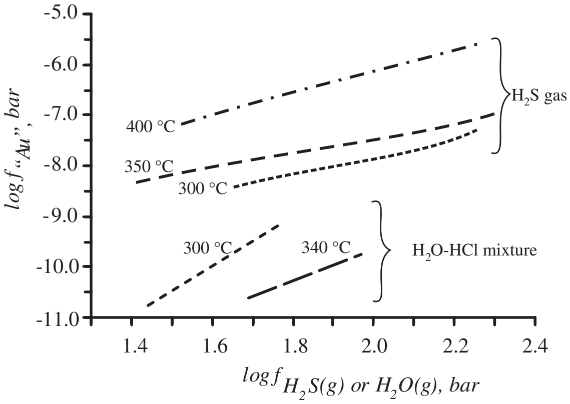

Fig. 10. A comparison of the solubility of gold in H_2O–HCl vapor mixtures (at $f_{HCl} = 0.065$ bar) measured by Archibald et al. (2001) with that in H_2S gas determined in this study. The solubility of Au in H_2O–HCl vapor mixtures is controlled by the formation of a hydrated gold chloride complex $AuCl \cdot (H_2O)_n$ with $n = 3$–5, and that in H_2S gas by the formation of the solvated sulfide or bisulfide complexes $AuS \cdot (H_2S)_n$ or $AuHS \cdot (H_2S)_n$ with $n = 1$–2.2.

temperature over the range of temperatures investigated (300–400 °C). However, the solvation number of gold chloride species dissolved in H_2O–HCl gas mixtures is greater ($n = 3$–5) than for species dissolved in H_2S gas ($n = 1$–2). Consequently, the solubility of gold as a chloride complex in natural chloride-bearing vapors will increase more rapidly with pressure than in an H_2S-bearing system. On the other hand, the gold solvation number of $AuCl \cdot (H_2O)_n$ decreases with decreasing temperature between 360 and 300 °C, whereas that of $AuS \cdot (H_2S)_n$ or $AuHS \cdot (H_2S)_n$ remains constant.

4.6. The capacity of natural H_2S-bearing vapor to transport gold

In order to evaluate the possible effect of H_2S complexation and solvation on the transport of gold in the vapor phase, we have calculated the likely concentration of gold in a hypothetical hydrothermal vapor. We have assumed that the vapor phase is produced by open system boiling, at a temperature of 400 °C, of a fluid analogous to that exsolved from a felsic calc-alkaline magma. The fluid has a salinity of 2 m NaCl, which is similar to that exsolved from the magma in Bingham porphyry (e.g., Redmond et al., 2004) and predicted on theoretical grounds by Burnham (1979). The H_2S concentration was assumed to be 0.1 m, based on the composition of typical geothermal waters and a correction to account for the dependence of the latter on temperature (Barnes and Seward, 1997). The data of Suleimenov and Krupp (1994) for the system H_2O–H_2S–NaCl were used to establish the partitioning of H_2S between liquid and vapor at 400 °C. The solubility of gold was assumed to be controlled by reaction (13) (reaction (14) would have yielded an identical result) and redox conditions buffered by the pair H_2S/S (i.e., between those of the hematite-magnetite and quartz–fayalite–magnetite buffers); note that Au solubility increases with increasing fO_2 (reaction 11).

Based on the above assumptions we calculated that after 0.1% boiling the mole fraction of H_2S in the vapor was effectively 1 (the P–T–X properties of the fluids were estimated from data for the NaCl–H_2O system reported by Sourirajan and Kennedy, 1962) and after 1% boiling had decreased to 0.18 (Fig. 11a). At these mole fractions of H_2S, the corresponding concentrations of gold are 90 and 2 ppb, respectively (Fig. 11b). For comparison, the time required to form a hydrothermal deposit containing 50 tons

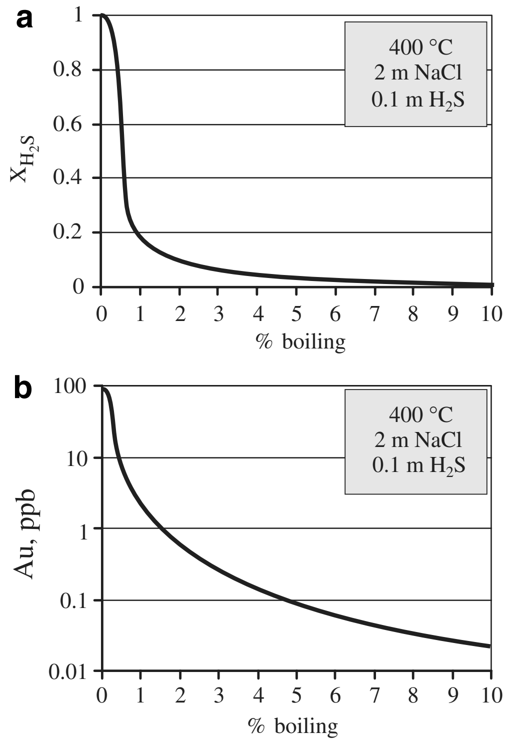

Fig. 11. The calculated mole fraction of H_2S in the vapor phase (a) and the calculated solubility of Au in the vapor phase (b) as a function of the extent of boiling of a 2 m NaCl aqueous liquid at 400 °C initially containing 0.1 m H_2S.

of gold (which is within the size range of numerous economic deposits) from a fluid with a concentration 1 ppb Au is 43 Ka assuming a depositional efficiency of 50% and a discharge rate similar to that of modern geothermal systems (e.g., 75 kg/s—Waiotapu; Henley, 1985). This time period is much less than the lifespan of many gold-depositing hydrothermal systems, e.g., the duration of the Far South-East-Lepanto system was about 300 ka (Arribas et al., 1995). Our calculations therefore show that it is possible for boiling to produce a vapor with the concentration of H_2S needed to economically transport significant quantities of gold but only if the proportion of vapor relative to that of the pre-boiled liquid is small.

5. CONCLUSIONS

The results of this experimental study support suggestions of other researchers that complexation with reduced sulfur may play an important role in the transport of gold in the vapor phase of hydrothermal systems. The solubility of Au in hydrogen sulfide gas can reach values of 1.4 ppb (wt.) at 300 °C, 8 ppb at 350 °C and 95 ppb at 400 °C, and we propose that this solubility is governed by the formation of a H_2S-solvated gaseous complex having the form $AuS\cdot(H_2S)_n$ or $AuHS\cdot(H_2S)_n$, where n is between 1 and 2 at temperatures ranging from 300 to 400 °C and pressures up to 230 bars. Although the experiments described here were not carried out at conditions directly applicable to nature, they do provide strong evidence that H_2S can play a major role in dissolving gold in hydrothermal vapors and that this role may be key to understanding the genesis of porphyry and epithermal gold deposits.

ACKNOWLEDGMENTS

This paper benefited considerably from thoughtful reviews by D.C. McPhail and two anonymous GCA referees. Financial support for the study was provided by grants from DIVEX, FQRNT and NSERC to A.E.W.-J.

REFERENCES

Archibald S. M., Migdisov A. A., and Williams-Jones A. E. (2001) The stability of Au–chloride complexes in water vapor at elevated temperatures and pressures. *Geochim. Cosmochim. Acta* **65**, 4413–4423.

Archibald S. M., Migdisov A. A., and Williams-Jones A. E. (2002) An experimental study of the stability of copper chloride complexes in water vapor at elevated temperatures and pressures. *Geochim. Cosmochim. Acta* **66**, 1611–1619.

Arribas, Jr., A., Hedenquist J. W., Itaya T., Okada T., Concepcion R. A., and Garcia, Jr., J. S. (1995) Contemporaneous formation of adjacent porphyry and epithermal Cu–Au deposits over 300 ka in northern Luzon. *Philippines Geol.* **23**, 337–340.

Barnes H. L., and Seward T. M. (1997) Geothermal systems and mercury deposits. In *Geochemistry of Hydrothermal Ore Deposits*, 3rd ed. (ed. H. L. Barnes), pp. 699–736.

Benning L. G., and Seward T. M. (1996) Hydrosulphide complexing of Au(I) in hydrothermal solutions from 150–400 °C and 500–1500 bar. *Geochim. Cosmochim. Acta* **60**, 1849–1871.

Binnewies M., and Milke E. (1999) *Thermochemical Data of Elements and Compounds*. Wiley-VCH, Weinheim, New York, 928 pp.

Burnham C. W. (1979) Magmas and hydrothermal fluids. In *Geochemistry of Hydrothermal Ore Deposits*, 2nd ed. (ed. H. L. Barnes), pp. 71–136.

Dennis Jr., J. E., Woods D. J. (1987) *New Computing Environments: Microcomputers in Large-Scale Computing* (ed. A. Wouk). SIAM, pp. 116–122.

Fanelli R. (1949) Solubility of hydrogen sulfide in sulfur. *Ind. Eng. Chem.* **41**, 2031–2033.

Féher F., and Winkhaus G. (1957) Zur termochemie der Sulfane: Bildungsenthalpien und Bindungsenergien. *Z. Anorg. Allgem. Chem.* **292**, 210–223.

Hayashi K.-I., and Ohmoto H. (1991) Solubility of gold in NaCl- and H_2S bearing aqueous solutions at 250–350 °C. *Geochim. Cosmochim. Acta* **55**, 2111–2126.

Heinrich C. A., Ryan C. G., Mernagh T. P., and Eadington P. J. (1992) Segregation of ore metals between magmatic brine and vapor: a fluid inclusion study using PIXE microanalysis. *Econ. Geol.* **87**, 1566–1583.

Heinrich C. A., Guenter D., Audetat A., Ulrich T., and Frischknecht R. (1999) Metal fractionation between magmatic brine and vapor, determined by microanalysis of fluid inclusions. *Geology* **27**, 755–758.

Henley R. W. (1985) Geothermal framework for epithermal deposits. In *Reviews in Economic Geology, Vol. 2: Geology and Geochemistry of Epithermal Systems* (eds. B. R. Berger and P. M. Bethke). pp. 1–25.

Loucks R. R., and Mavrogenes J. A. (1999) Gold solubility in supercritical hydrothermal brines measured in synthetic fluid inclusions. *Science* **284**, 2159–2163.

Migdisov Art. A., Suleimenov O. M., and Alekhin Yu. V. (1998) Experimental study of polysulfane stability in gaseous hydrogen sulfide. *Geochim. Cosmochim. Acta* **62**, 2627–2635.

Migdisov A. A., Williams-Jones A. E., and Suleimenov O. M. (1999) Solubility of chlorargyrite (AgCl) in water vapor at elevated temperatures and pressures. *Geochim. Cosmochim. Acta* **63**, 3817–3827.

Migdisov Art. A., and Williams-Jones A. E. (2005) An experimental study of cassiterite solubility in HCl-bearing water vapour at temperatures up to 350 °C. Implications for tin ore formation. *Chem. Geol.* **217**, 29–40.

Mills K. C. (1974) *Thermodynamic Data for Inorganic Sulphides, Selenides and Tellurides*. National Physical Laboratory, Teddington, Middlesex, London, Butterworths, 844 pp.

Nelder J. A., and Mead R. (1965) A simplex method for function minimization. *Comput. J.* **7**, 308–313.

Pokrovski G. S., Borisova A. Yu., and Harrichoury J. C. (2006) The effect of sulfur on vapor–liquid partitioning of metals in hydrothermal systems: an experimental batch-reactor study. *Geochim. Cosmochim. Acta* **70**, A498.

Rau H., Kutty T. R. N., and Guedes de Carvalho J. R. F. (1973) Thermodynamics of sulphur vapour. *J. Chem. Thermodynamics* **5**, 833–844.

Rau H., and Mathia W. (1982) Equation of state for gaseous H_2S. *Ber. Bunsengesellschaft Phys. Chem.* **86**, 108–109.

Redmond P. B., Einaudi M. T., Inan E. E., Landtwing M. R., and Heinrich C. A. (2004) Copper deposition by fluid cooling in intrusion-centered systems: new insights from the Bingham porphyry ore deposit, Utah. *Geology* **32**, 217–220.

Rempel K. U., Migdisov A. A., and Williams-Jones A. E. (2006) The solubility and speciation of molybdenum in water vapor at elevated temperatures and pressures: implications for ore genesis. *Geochim. Cosmochim. Acta* **70**, 687–696.

Sandler S. I. (1989) *Chemical and Engineering Thermodynamics*. Wiley, New York, 622 pp.

Smoes S., and Drowart J. (1968) Mass-spectrometric determination of the dissociation energy of the molecule AuMn. *Chem. Commun.* **9**, 534–535.

Sourirajan S., and Kennedy G. C. (1962) The system H_2O–NaCl at elevated temperatures and pressures. *Am. J. Sci.* **260**, 115–141.

Stefansson A., and Seward T. M. (2004) Gold(I) complexing in aqueous sulfide solutions to 500 °C and 500 bar. *Geochim. Cosmochim. Acta* **68**, 4121–4143.

Steudel R. (2003) Inorganic polysulfanes H_2S_n with $n > 1$. *Top. Curr. Chem.* **231**, 99–125.

Suleimenov O. M., and Ha T.-K. (1998) Ab initio calculation of the thermochemical properties of polysulfanes (H_2S_n). *Chem. Phys. Lett.* **290**, 451–457.

Suleimenov O. M., and Krupp R. E. (1994) Solubility of hydrogen sulfide in pure water and in NaCl solutions, from 20 to 320 °C and at saturation pressures. *Geochim. Cosmochim. Acta* **58**, 2433–2444.

Symonds R. B., and Reed M. H. (1993) Calculation of multicomponent chemical equilibria in gas–solid–liquid systems: calculation methods, thermochemical data, and applications to studies of high-temperature volcanic gases with examples from Mount St.. *Helens. Am. J. Sci.* **293**, 758–864.

Tagirov B. R., Salvi S., Schott J., and Baranova N. N. (2005) Experimental study of gold–hydrosulphide complexing in aqueous solutions at 350–500 °C, 500 and 1000 bars using mineral buffers. *Geochim. Cosmochim. Acta* **69**, 2119–2132.

Taran Yu. A., Bernard A., Gavilanes J.-C., and Africano F. (2000) Native gold in mineral precipitates from high-temperature volcanic gases of Colima volcano, Mexico. *Appl. Geochem.* **15**, 337–346.

Wiewiorowski T. K., and Touro F. J. (1966) Molten sulfur chemistry. I. Chemical equilibriums in pure liquid sulfur. *J. Phys. Chem.* **70**, 234.

Williams-Jones A. E., and Heinrich C. A. (2005) Vapor transport and the formation of magmatic-hydrothermal ore deposits. *Econ. Geol.* **100**, 1287–1312.

Williams-Jones A. E., Migdisov A. A., Archibald S. M., Xiao Z. (2002) Vapor-transport of ore metals. In *Water–Rock Interaction, Ore Deposits, and Environmental Geochemistry: A Tribute to David A. Crerar* (eds. R. Hellmann and S. A. Wood). The Geochemical Society, Special Publication No. 7, pp. 279–305.

Zakaznova-Iakovleva V. P., Migdisov A. A., Suleimenov O. M., Williams-Jones A. E., and Alekhin Yu. V. (2001) An experimental study of stibnite solubility in gaseous hydrogen sulfide from 200 to 320 °C. *Geochim. Cosmochim. Acta* **65**, 289–298.

Associate editor: Jeremy Fein